Hindawi
Molecular Imaging
Volume 2022, Article ID 1076444, 11 pages
https://doi.org/10.1155/2022/1076444

Research Article

Neuroinflammation in Low-Level PM2.5-Exposed Rats Illustrated by PET via an Improved Automated Produced [^{18}F]FEPPA: A Feasibility Study

Mei-Fang Cheng,[1,2] Tsun-Jen Cheng,[2] Yue Leon Guo,[2] Ching-Hung Chiu,[1] Hung-Ming Wu,[3] Ruoh-Fang Yen,[1,4] Ya-Yao Huang,[1,4,5] Wen-Sheng Huang,[6,7,8] and Chyng-Yann Shiue[1,4,9]

[1]*Department of Nuclear Medicine, National Taiwan University Hospital, Taipei, Taiwan*
[2]*Institute of Environmental and Occupational Health Sciences, National Taiwan University, Taipei, Taiwan*
[3]*Department of Neurology, Changhua Christian Hospital, Taiwan*
[4]*Molecular Imaging Center, National Taiwan University, Taipei, Taiwan*
[5]*Institute of Medical Device and Imaging, National Taiwan University College of Medicine, Taipei, Taiwan*
[6]*Department of Nuclear Medicine, Taipei Veterans General Hospital, Taipei, Taiwan*
[7]*Department of Nuclear Medicine, Taipei Medical University Hospital, Taipei, Taiwan*
[8]*Department of Nuclear Medicine, Cheng-Hsin General Hospital, Taipei, Taiwan*
[9]*PET Center, Department of Nuclear Medicine, Tri-Service General Hospital, Taiwan*

Correspondence should be addressed to Ya-Yao Huang; yayaohuang@ntu.edu.tw, Wen-Sheng Huang; wshuang01@gmail.com, and Chyng-Yann Shiue; shiue@ntuh.gov.tw

Received 1 December 2021; Revised 10 April 2022; Accepted 18 May 2022; Published 7 June 2022

Academic Editor: Henry VanBrocklin

Background. [^{18}F]FEPPA is a potent TSPO imaging agent that has been found to be a potential tracer for imaging neuroinflammation. In order to fulfill the demand of this tracer for preclinical and clinical studies, we have developed a one-pot automated synthesis with simplified HPLC purification of this tracer, which was then used for PET imaging of neuroinflammation in fine particulate matter- (PM2.5-) exposed rats. *Results*. Using this automated synthesis method, the RCY of the [^{18}F]FEPPA was 38 ± 4% (n = 17, EOB) in a synthesis time of 83 ± 8 min from EOB. The radiochemical purity and molar activities were greater than 99% and 209 ± 138 GBq/μmol (EOS, n = 15), respectively. The quality of the [^{18}F]FEPPA synthesized by this method met the U.S. Pharmacopoeia (USP) criteria. The stability test showed that the [^{18}F]FEPPA was stable at 21 ± 2°C for up to 4 hr after the end of synthesis (EOS). Moreover, microPET imaging showed that increased tracer activity of [^{18}F]FEPPA in the brain of PM2.5-exposed rats (n = 6) were higher than that of normal controls (n = 6) and regional-specific. *Conclusions*. Using the improved semipreparative HPLC purification, [^{18}F]FEPPA has been produced in high quantity, high quality, and high reproducibility and, for the first time, used for PET imaging the effects of PM2.5 in the rat brain. It is ready to be used for imaging inflammation in various clinical or preclinical studies, especially for nearby PET centers without cyclotrons.

1. Introduction

Neuroinflammation is an inflammatory and adaptive response within the central nervous system (CNS) [1] and is the driving force for disease progression, such as Alzheimer's disease (AD) [2], major depressive disorder [3], schizophrenia [4], and brain injuries [4]. Activated in response to neuropathologies [5, 6], microglia and astrocytes have been known to be the predominant mediators during the neuroinflammatory process. The transmembrane domain protein, translocator protein-18 kDa (TSPO), is variously expressed throughout the body and has low

expression within the brain [7–9]. However, TSPO levels are significantly increased in the brain when microglia and astrocyte are activated [10, 11]. Recently, the results of meta-analyses of TSPO levels in mild cognitive impairment and AD further supported the association of increased neuroinflammation during the progression of mild cognitive impairment and AD, relative to healthy controls [12]. In addition to CNS, an increase in TSPO expression has also been seen in a wide variety of malignant human cells and tissues including brain cancers [13, 14], prostate cancers [15, 16], colon cancers [17–19], breast cancers [20, 21], esophageal cancers [22], endometrial carcinomas [23], ovarian cancers, and hepatic carcinomas [24]. Albeit its lack of specificity to activated microglia, the TSPO levels may at times reflect neuroinflammation *in vivo* [10].

Exposure to fine particulate matter (PM2.5) has been linked to adverse neurological and behavioral health effects, including increased risk for cognitive decline (AD) [25, 26], Parkinson's disease [27], ischemic stroke [28], and anxiety or depression [29, 30] in epidemiology studies. Increases in neuroinflammation and oxidative stress have been identified as putative mechanisms by which fine PM2.5 may impair central nervous system function [31, 32], an example of which occurs when exacerbated and unregulated microglial proinflammatory responses play crucial factors involved in brain damage [33]. Chronic activation of the microglia (reactive microgliosis) has been implicated in neuronal injury and neuronal damage after exposure to PM2.5 [34]. One hallmark of microglial activation is the overexpression of TSPO [35, 36]. To the best of our knowledge, the application of a TSPO imaging agent for studying the effects of PM2.5 on human health has not been reported. Thus, we have developed an one-pot automated synthesis of [^{18}F]FEPPA, a potent TSPO imaging agent, and used it to investigate (1) whether PET imaging can noninvasively detect microglia activation after chronic subacute ambient PM2.5 exposure in spontaneous hypertensive rats and (2) whether there is a specific pattern of microglia activation in the brain after chronic subacute ambient PM2.5 exposure.

The first TSPO PET ligand, [^{11}C]PK-11195 was synthesized more than two decades ago [37–39]. However, its utility was limited due to its low brain penetration, high nonspecific binding, high plasma protein binding, and short half-life (for review, see [37, 38]). Therefore, several second-generation ^{18}F-labelled TSPO PET ligands, including [^{18}F]FEPPA [40–43], [^{18}F]FEDAA1106 [44, 45], [^{18}F]DPA-714 [46, 47], and [^{18}F]PBR06 [48, 49] have been developed (for review, see [50, 51]). Recently, a novel third-generation TSPO PET ligand, [^{18}F]GE180 was developed [52–54] and proved to be useful for TSPO imaging [53, 55, 56]. However, its application for neuroimaging is very limited as it suffers from very low brain penetration, similar to that of [^{11}C]PK-11195. Specifically, in humans, the VT of [^{18}F]GE180 is 20-fold lower than that of [^{11}C]PRB28 [57]. Among these tracers, [^{18}F]-N-(2-(2-fluoroethoxy)benzyl)-N-(4-phenoxypyridin-3-yl)acetamide ([^{18}F]FEPPA) shows outstanding properties regarding affinity, stability, lipophilicity, and radiosynthesis [43] and has been used in several preclinical [40, 58, 59] and clinical settings [60–66]. In order to facilitate the usefulness of [^{18}F]FEPPA in both preclinical and clinical studies, it is imperative to have a fully automated, simple, high yield, and reliable manufacturing process method available for the production of this tracer. Thus, we have adopted Wilson's method [43], with some modifications, to fully automate the synthesis of this potent TSPO imaging agent using a TRACERlab Fx_{FN} module (GE Healthcare, Milwaukee, WI) with ethanol and water for purification in high quality and high reproducibility. Vignal et al. reported a similar synthesis using ethanol, water, and phosphoric acid for purification of [^{18}F]FEPPA [42]. We report herein (1) a one-pot automated synthesis of [^{18}F]FEPPA with a simplified HPLC purification, (2) the USP compliant QC and stability tests of [^{18}F]FEPPA, and (3) microPET imaging of [^{18}F]FEPPA in PM2.5-exposed rats.

2. Materials and Methods

The precursor (N-[[2-[2-[[(4-methylphenyl)sulfonyl]oxy]ethoxy]phenyl]methyl]-N-(4-phenoxy-3-pyridinyl) acetamide, TsEPPA, 1) and the nonradioactive authentic sample N-(2-(2-fluoroethoxy)benzyl)-N-(4-phenoxypyridin-3-yl) acetamide (FEPPA, 2) were purchased from ABX Advanced Biochemicals (Radeberg, Germany). All other chemicals and solvents were purchased from either Sigma-Aldrich (Milwaukee, WI, USA) or Acros Organics (Morris Plains, NJ, USA) and used without further purification. [^{18}O]O_2H (>98% enriched) was purchased from Rotem Industries (Beer Sheva, Israel). Aqueous [^{18}F]Fluoride was produced in our PET Trace cyclotron (GE Medical Systems, Uppsala, Sweden) via ^{18}O(p, n)^{18}F nuclear reaction. All Sep-Pak® cartridges were purchased from Waters Associates (Milford, MA, USA).

2.1. Automated Radiosynthesis. The [^{18}F]FEPPA (2) was produced by automated synthesis via fluorination of the TsEPPA (1) with K[^{18}F]/$K_{2.2.2}$ followed by purification with HPLC, to give [^{18}F]FEPPA (2) as previously reported (Scheme 1) [43].

The [^{18}F]FEPPA (2) was produced by automated synthesis using a modified TRACERlab Fx_{FN} module (GE Healthcare, Milwaukee, WI; Figure 1). Briefly, fluorination of TsEPPA (1) with K[^{18}F]/$K_{2.2.2}$ in anhydrous MeCN at 70°C for 20 min gave the crude product (1) (Scheme 1). After dilution with H_2O, the crude product (1) was purified with a semipreparative HPLC (Waters Xterra RP-18, 10 μm, 10 × 250 mm, 35% aqueous ethanol in water for injection, 254 nm, 4 mL/min). The fraction containing [^{18}F]FEPPA (2) was collected, reformulation, and sterile filtration to provide (2) with <10% of ethanol concentration for PET imaging of the effects for PM2.5 in rats. Please refer to Supplementary data for detailed steps of radiosynthesis.

2.2. Quality Control (QC) and Stability Tests of the [^{18}F]FEPPA (2). The radiochemical purity, chemical purity, and molar activity of 2 were analyzed with an HPLC system (Agilent 1100 series) equipped with a Bioscan FC3300 flow count radioactivity detector (2″ × 2″ pinhole) and a UV

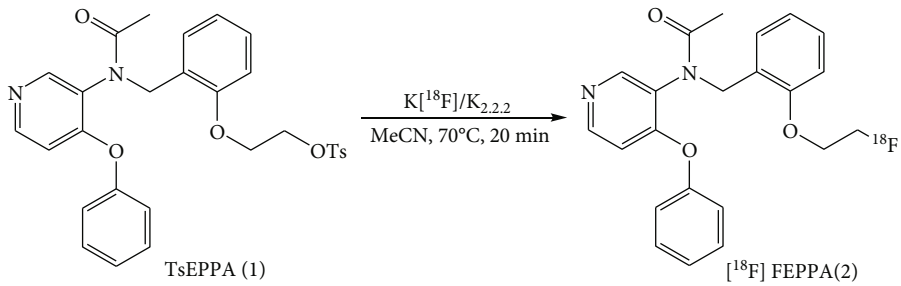

Scheme 1: Radiosynthesis of the [^{18}F]FEPPA (2).

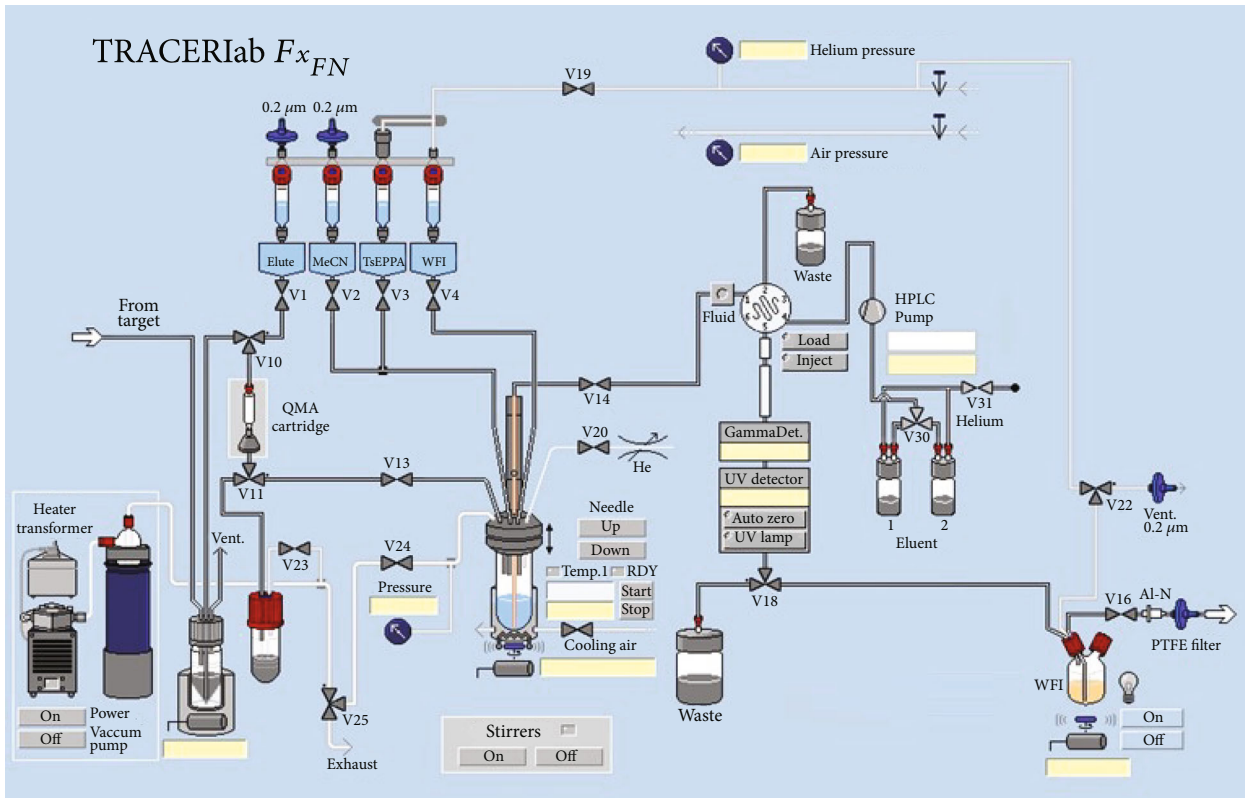

Figure 1: Modified TRACERLab Fx$_{FN}$ module for the [^{18}F]FEPPA (2) radiosynthesis.

detector (254 nm) using a Waters Xterra column (RP-18, 5 μm, 4.6 × 250 mm) with 50% aqueous MeCN as the eluent and a flow rate of 1.0 mL/min. The chemical identity of the [^{18}F]FEPPA (2) was confirmed by coinjection with a nonradioactive authentic FEPPA. The radiochemical impurity of 2 was further analyzed with radio TLC (Silica gel 60 F254 plate, 10 cm, ethyl acetate/hexane (3/1)) and detected with a Raytest miniGita radio-TLC scanner (Raytest, Straubenhardt, Germany). Please refer to Supplementary data and Figure S1 for details.

Other items of QC test and corresponding criteria of 2 were set according to the U.S. Pharmacopoeia (USP) for radiopharmaceuticals [67], which included visual inspection, pH, half-life of radionuclide, radionuclidic purity, radiochemical purity, chemical purity, residual $K_{2.2.2}$, residual solvents, bacterial endotoxins, filter integrity, and sterility test.

The stability of 2 at 21 ± 2°Cwas monitored with both TLC and HPLC as described above for up to 4 hr after EOS.

2.3. MicroPET Imaging of the [^{18}F]FEPPA (2) Injection in Rats Exposed to Ambient Fine Particulate Matter (PM2.5)

2.3.1. Animals. Male spontaneously hypertensive rats (7-week-old, average weight of 350 g, $n = 12$) were obtained from the National Laboratory Animal Center (Taipei, Taiwan) and were randomly classified into ambient fine PM exposure group (aerodynamic diameter of <2.5 μm, PM2.5; $n = 6$) and high-efficiency particulate air- (HEPA-)-filtered air (FL, $n = 6$) conditions group using Taipei Air Pollution Exposure System (TAPES) for health effects [68, 69] for 24 hours per day, 7 days per week, for a total of 6 months. The coarse (PM2.5-10) and fine (PM2.5) size concentrations

Table 1: The QC tests of the [^{18}F]FEPPA (2).

Items tested	Acceptance criteria			
Visual inspection	Clear, colorless solution	Pass	Pass	Pass
pH value	5-8	7	7	7
Residual $K_{2.2.2}$ (μg/mL)	<50	<50	<50	<50
Radionuclidic purity (%)	>99.5	99.93	99.96	99.62
Half-life (min)	110 ± 5	108	115	115
Radiochemical identity (min)	$\lvert R_t\text{-}R_t$ (reference)$\rvert \leq 0.5$	0.02	0.00	0.07
Radiochemical purity (%)	>90	99.9	99.8	99.8
Residual solvent analysis	EtOH < 10% Acetone < 0.5% MeCN < 0.04%	4.6849% 0.1454% 0.0100%	0.1673% 0.0324% 0.0014%	2.2298% 0.0010% 0.0008%
Residual [^{18}F]Fluoride (%)	<5	0.01	0.02	0.59
Bacterial endotoxins (EU/V)	<175	<17.5	<17.5	<17.5
Filter integrity test (psi)	>45	48.5	46.6	46.0
Sterility test	Sterile	Sterile	Sterile	Sterile

constituted 0.4 and 99.6% of the whole-body exposure system [70]. Therefore, the rats were mostly exposed to PM2.5. The rats were housed in ventilated cages under a conditioned environment as illustrated in our previous studies [68]. Lab diet and water were provided *ad libitum* during the study. The animal experiments adhered to protocols of the Institutional Animal Care and Use Committee (IACUC) of the Laboratory Animal Center at National Taiwan University (ACUC no: 20160025).

At the end of exposure, [^{18}F]FEPPA microPET/CT brain scan was performed for each rat to assess the degree of neuroinflammation. During scanning, rats were anesthetized by passive inhalation of a mixture of isoflurane (5% for induction and 2% for maintenance) in oxygen, followed by a bolus tail vein injection of 24 ± 10 MBq, $n = 6$) of (2). Brain transmission and emission scans of rats were acquired with a small animal Argus PET/CT scanner (SEDECAL, Madrid, Spain). Ten minutes posttail vein injection of (2), static sinograms were produced for 30 min for each organ of interest. Images were analyzed using commercial PMOD software (PMOD Technologies LLC, version 3.6, Zurich, Switzerland) after coregistration the microCT images to the innate MR atlas. Regional brain radioactivity concentrations (MBq/cm^3) were normalized to the injected activity (MBq) and the weight (g) of organ to yield a semiquantitative measurement of radiotracer binding, standardized uptake value (SUV) [71]. The mean SUV of each brain region (volume of interest, VOI) such as the whole brain, frontal lobe, parietal lobe, insular lobe, occipital lobe, midbrain, temporal lobe, hippocampus, retrosplenial cortex in the temporal lobes, and cerebellum were calculated and analyzed.

2.4. Immunohistochemical Analysis. After PET image acquisition, all rats were sacrificed. The brain tissues were processed using an automated tissue processor (Shandon Excelsior, Thermo Scientific, UK), embedded in paraffin, and cut at a thickness of 3-5 μm for immunohistochemical (IHC) staining. Ionized calcium binding adaptor molecule (Iba1) is a macrophage-specific calcium-binding protein, participating in membrane ruffling and phagocytosis in the activated microglia. For Iba1 staining, brain tissues were stained against the activated microglial marker Iba1 (GeneTex, San Antonio, TX, USA) [72]. The percentage of areas occupied by the stained nuclei of activated microglia at 40x high power field (0.26 mm/pixel) in the hippocampal region of the rats was calculated using a digital slide scanner (MoticEasyScan, Motic®, Canada). The brain tissues were examined by a histopathologist blinded to the exposure data.

2.5. Statistical Analysis. Data was expressed as mean ± standard deviation (SD). Wilcoxon rank sum test was used to compare different regions of brain in PM2.5 and FL rats. $P < 0.05$ was regarded as statistically significant. Statistical analyses were performed using JMP®, version 10 statistical software package (SAS Institute Inc., Cary, NC, USA).

3. Results

3.1. A One-Pot Automated Synthesis of the [^{18}F]FEPPA (2) Using a Modified Fx_{FN} Module. In this paper, we presented the detailed automated production of [^{18}F]FEPPA along with a full set of quality control specifications and results in USP compliance. Using this modified purification method, we were able to routinely produce 2 with a Fx_{FN} module in 38 ± 4% yield (EOB, $n = 17$) in a synthesis time of 83 ± 8 min from EOB. Typically, starting with 35 GBq of [^{18}F]Fluoride, 8 GBq of 2 was produced at EOS. Both the chemical and radiochemical purities of 2 were greater than 90% with a molar activity of 209 ± 138 GBq/μmol ($n = 15$, EOS) and were used for PET imaging of the effects of PM2.5 in rats.

The QC test results of 2 are tabulated in Table 1. Moreover, the stability test showed that 2 synthesized by this method was stable at room temperature (21 ± 2°C) for up to 4 hr after EOS (Table 2). Detailed QC data for [^{18}F]FEPPA produced using our method disclosed herein are shown in supplementary data.

Table 2: Stability of three consecutive productions of the [^{18}F]FEPPA (2) ($n = 3$).

Items tested	Acceptance criteria	Elapsed time (hr)	Run 1	Run 2	Run 3
Radiochemical purity (%)	>90%	0	99.9	99.8	99.8
		2	99.0	99.3	98.6
		4	98.9	99.4	97.7
Residual [^{18}F]Fluoride (%)	<5%	0	0.01	0.02	0.59
		2	0.34	0.73	1.01
		4	1.04	0.23	1.89

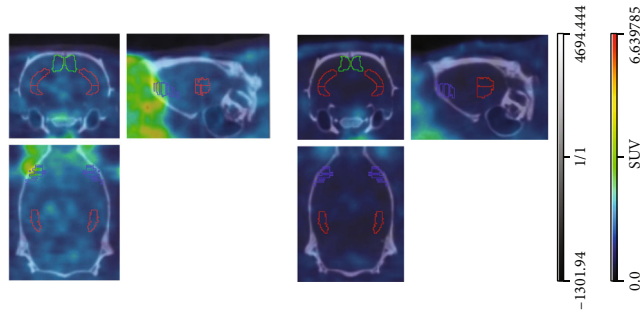

(a) (b)

Figure 2: Representative imaging of coronal, sagittal, and axial sections of rat brain exposed to ambient PM2.5 ((a) PM2.5, left panel) versus filtered air ((b) FL, right panel).

3.2. MicroPET Imaging of the [^{18}F]FEPPA (2) Injection in Rats Exposed to Ambient Fine Particulate Matter (PM2.5). The mean mass concentration of PM2.5 during the exposure period was $10.8 \pm 3.8\,\mu g/m^3$. The predominant chemical composition of the trapped particles in the PM group was sulfur (16.0% of mean PM2.5 concentration), potassium (1.2%), and iron (0.6%), similar to that in previous PM exposure data [68, 70]. There was no significant alterations in the weight of the rats after ambient PM2.5 exposure between the PM2.5 and FL groups.

Typical whole-brain biodistribution of [^{18}F]FEPPA in the PM2.5 and FL rats was depicted in Figure 2. Increased tracer activity of [^{18}F]FEPPA in selected brain regions was shown in Table 3 and Figure 3 and expressed as SUV mean.

Specifically, significant increased [^{18}F]FEPPA tracer activity was observed in the temporal lobe of the PM2.5 compared to that of the FL rats ($P = 0.04$), especially in the hippocampus (Figure 2, red contour, $P = 0.01$) and retrosplenic region (Figure 2, green contour, $P = 0.03$). A trend of increased tracer activity was found at insular areas (Figure 2, indigo contour) and frontal lobe (not shown) in the PM2.5 rats, but not reaching statistical difference (Table 3).

3.3. Immunohistochemical (IHC) Staining of the Rat Brain. The IHC staining of the hippocampus showed that the % of area with Iba1 staining at 40x high power field were $0.130 \pm 0.017\%$ in the FL group vs. $0.313 \pm 0.081\%$ in the PM2.5 group (Figure 4, $P = 0.05$).

There is a trend for higher Iba1 staining (brown-colored nuclei, red arrows) in the hippocampus of PM rats (a) compared to the FL group (b), but the difference is not statistically significant (staining area of $0.313 \pm 0.081\%$ vs. $0.130 \pm 0.017\%$, $P = 0.05$ (c)).

Table 3: MicroPET Imaging of the [^{18}F]FEPPA (2) in ambient PM2.5-exposed ($n = 6$) versus filtered air-exposed ($n = 6$) rats.

Region	PM (SUV mean)	FA (SUV mean)	P value
Whole brain	0.85 ± 0.02	0.78 ± 0.03	0.03*
Frontal lobe	0.92 ± 0.02	0.87 ± 0.02	0.047
Parietal lobe	0.73 ± 0.04	0.75 ± 0.03	NS
Insular lobe	0.93 ± 0.04	0.83 ± 0.02	0.047
Occipital lobe	0.64 ± 0.04	0.68 ± 0.03	NS
Midbrain	0.80 ± 0.04	0.81 ± 0.04	NS
Olfactory bulb	0.99 ± 0.04	1.06 ± 0.06	NS
Temporal lobe	0.78 ± 0.02	0.71 ± 0.03	0.04*
Hippocampus	0.73 ± 0.02	0.66 ± 0.02	0.01*
Retrosplenial cortex	0.83 ± 0.04	0.71 ± 0.04	0.03*
Cerebellum	0.85 ± 0.04	0.86 ± 0.05	NS

Abbreviations: FA: filtered air; NS: not significant; PM: particulate matter.

4. Discussion

[^{18}F]FEPPA is a potent TSPO imaging agent that has been found to be a potential tracer for imaging neuroinflammation. In order to fulfill the demand of this tracer for preclinical and clinical studies, we have developed a one-pot automated synthesis with simplified HPLC purification of this tracer, which was then, for the first time used for PET imaging of the effects of PM2.5 in rats.

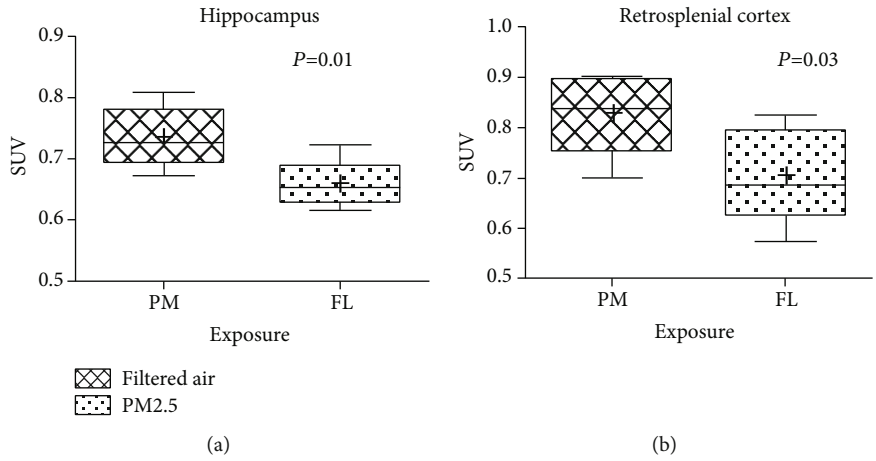

Figure 3: Tracer distribution of the [^{18}F]FEPPA (2) in the hippocampus (a) and retrosplenial region (b) of the temporal lobes.

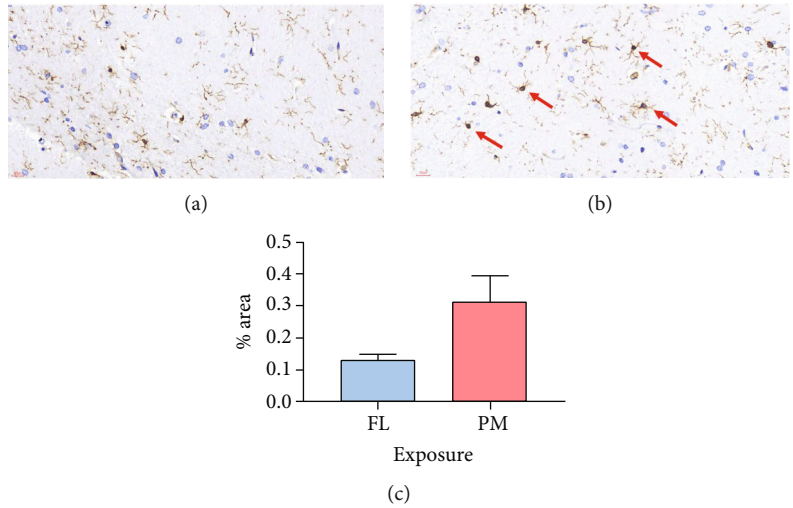

Figure 4: The immunostaining (brown-colored nuclei, red arrows) in the hippocampus of the PM rats (a), FL rats (b), and the differences between these two groups (c).

[^{18} F]FEPPA (2) has been synthesized by several methods in various radiochemical yields and radiochemical purities [42, 43, 58, 73]. Initially, 2 was synthesized manually by nucleophilic fluorination of the corresponding tosylate-precursor (TsEPPA, 1) with [^{18}F]Fluoride, followed by purification with HPLC, to give 2 in 71~85% yield (EOB) (Scheme 1) [43]. Later, several automated syntheses of 2 were reported [42, 58, 73] (Table 4).

However, most of these automated syntheses used toxic MeCN as the solvent for semipreparative HPLC purification, and thus, reformulation was necessary. As a result, we and others [42] have chosen to use aqueous ethanol as the mobile phase for purification of 2 with HPLC. The HPLC purification conditions of 2 have been optimized by using a Waters Xterra RP-18 column (10 μm, 10 × 25 mm) and eluting with different flow rates and different concentrations of aqueous ethanol as mobile phase (Figure S2). Although the retention time was slightly longer when separation was done using 35% instead of 40% EtOH, but because of practical considerations, including nonradioactive impurity separation and easy-to-prepare mobile phase (Figure S3), 35% EtOH at a flow rate of 4 mL/min was chosen as the best condition for purification 2 (Figure 5).

However, a small amount of [^{18}F]Fluoride was detected in the eluate, which may have had an impact on PET image quality [74]. Thus, the eluate was further passed through an Alumina-N cartridge and a PTFE sterile filter in series to remove the residual [^{18}F]Fluoride and resulted in the pure and sterile 2 in 38 ± 4% yield (EOB, $n = 17$) in a synthesis time of 83 ± 8 min from EOB, which is comparable to 2 synthesized by other methods (Table 4). For TSPO-targeting studies, the molar activity is recommended as high as possible as required for studies targeting receptors. Compared to previous published methods, our method achieved a reasonable and high molar activity of 209 ± 138 GBq/μmol, EOS ($n = 17$) as shown in Table 4. Quality control and stability tests confirmed that 2 synthesized by this method met the USP. As far as we know, our method is still the only to address residual [^{18}F]Fluoride concern during automated production, as well as the QC item of residual [^{18}F]Fluoride

Table 4: Synthesis of the [^{18}F]FEPPA (2) via various methods.

References	Radiofluorination condition				RCY (%, EOB)	Synthesis time (min)	Number of production	Molar activity (GBq/μmol)	Automate synthesizer	QC (EP or USP)	TLC
	Precursor weight (mg)	Solvent (mL)	Temperature (°C)	Time (min)							
Wilson et al. [43]	5	MeCN 0.7 mL	90	10	71–85	40–50	—	44~100	—	—	—
Vasdev et al. [58]	5	MeCN 0.75 mL	90	10	38 ± 10	36 ± 1	54	222 ± 148	Fx_{FN}	—	—
Berroterán-Infante et al. [73]	3.125	MeCN 0.5 mL	90	10	38 ± 3	30	15	241 ± 13	Nuclear Interface	EP	Y*
Vignal et al. [42]	5	MeCN 1 mL	90	10	48 ± 3	55	17	198 ± 125	AllInOne®	—	—
Zammit et al. [59]	2	MeCN 0.4 mL	90	10	41 ± 8	78 ± 4	—	751 ± 163	CPCU	—	—
Chang et al. [74]	5	MeCN 0.6 mL	90	10	50	80	8	149~217	Eckert-Ziegler modular system	—	—
This study	5	MeCN 1 mL	70	20	38 ± 4	83 ± 8	17	209 ± 138	Fx_{FN}	USP	Y

*No TLC data were provided.

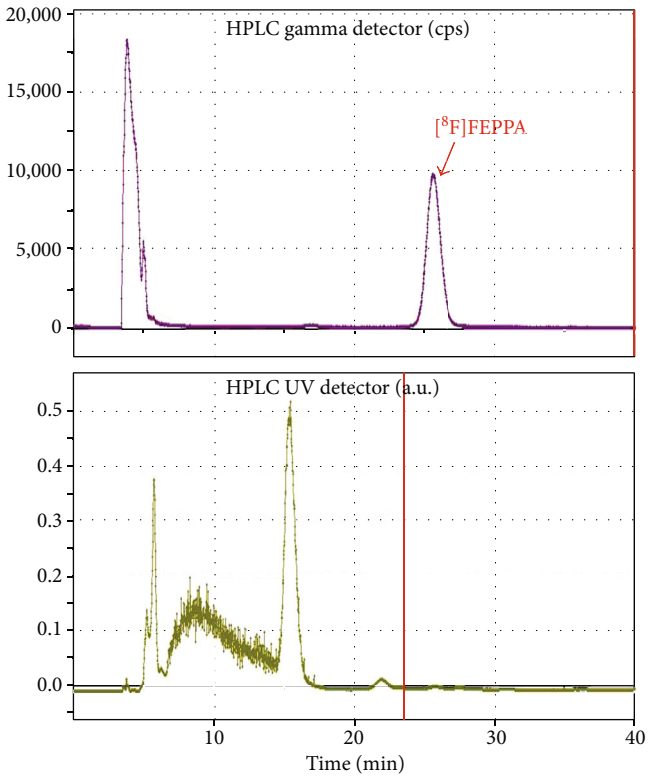

Figure 5: Representative semipreparative HPLC purification chromatogram of the [^{18}F]FEPPA (2).

determination using radio-TLC analysis, in order to achieve high quality of produced [^{18}F]FEPPA for preclinical or clinical studies.

PET imaging in rats showed that the whole-brain [^{18}F]FEPPA tracer activity of the PM2.5 rats was significantly higher than that of their age-matched FL rats. In addition, the brain tracer activity of [^{18}F]FEPPA was found to be regional-specific, and the difference was more pronounced in the temporal and insular lobes. In the temporal lobe, only the hippocampus and retrosplenial cortex showed statistical higher [^{18}F]FEPPA activity in the PM2.5 rats when compared to that of the FL rats (Table 3, Figure 3). A trend of increased tracer activity was found at both insular and frontal regions in the PM2.5 rats but did not reach a statistically significant difference.

The IHC staining results showed that although there was not a statistically significant difference in the hippocampus, a trend of increased Iba1 staining in the microglia cells was observed in the PM2.5 group compared to that of the filtered air group, which suggested that microglial activation and inflammation, especially in the temporal lobe, may play important roles in the response of the brain to traffic-related PM.

Taken collectively, we have developed an improved method to automatically produce [^{18}F]FEPPA in high quantity, high quality, and high reproducibility, and for the first time using it to noninvasively elucidate the microglial changes in different brain regions of rats after subchronic real-world exposure to ambient PM2.5. Our study confirmed that chronic subacute ambient PM2.5 exposure can lead to diffuse microglial activation. The brain area that was especially vulnerable to PM2.5 effects was the temporal lobe, particularly the hippocampus and retrosplenial cortex. These regions played crucial roles in memory, learning, and navigation, especially in the hippocampus. However, there are several limitations of the present rodent study. First, the limited sample size may influence the overall power of the test. On the other hands, this also suggests that with larger sample sizes, perhaps more brain regions will be affected, as we did observe a trend of increased [^{18}F]FEPPA activity

(not reaching statistical significance) in the insular and frontal regions of PM2.5 rats compared to their controls. Second, hypertensive rats were used in the current experiment, a subgroup that may be more vulnerable to fine PM exposure than normotensive rats. Spontaneous hypertensive rats were chosen since cardiovascular diseases are recognized as risk factors for developing neurodegenerative disease in humans and therefore may be more susceptible to traffic-related PM2.5 exposure. Third, blocking experiment using a nonradioactive FEPPA or other nonradioactive TSPO ligand was not performed in the current study. Nonetheless, [^{18}F]FEPPA is a relatively popular ligand that had been used in many preclinical and clinical studies [75, 76], including and not limited to psychiatric disorders [62, 77]. Various studies have also demonstrated that [^{18}F]FEPPA reliably binds to TSPO in the brain [78–80]. Lastly, not all regions of the brain were analyzed for Iba1 staining. Nevertheless, the areas of increased Iba1 staining were consistent with the [^{18}F]FEPPA PET findings.

5. Conclusions

With this one-pot automated synthesis and improved purification of the [^{18}F]FEPPA (2) using a Fx_{FN} Module, [^{18}F]FEPPA (2) can be produced with high quality, quantity, and reproducibility. PET imaging in rats exposed to low-level PM2.5 demonstrated that pulmonary exposure to fine PM may exert health effects on specific areas of the brain, including the hippocampus. The microglial activation and inflammation can be noninvasively evaluated and followed by [^{18}F]FEPPA PET imaging. The role of microglial response after low-level fine PM2.5 exposure warrants further investigation in humans. The applications of [^{18}F]FEPPA (2) for studying inflammation in the peripheral organs of animals and humans are in progress.

Data Availability

The datasets used and/or analyzed during the current study are available from the corresponding authors on reasonable request.

Ethical Approval

The animal experiments adhered to the Guide for the Care and Use of Laboratory Animals and were approved by the Laboratory Animal Center at National Taiwan University (Taipei, Taiwan).

Conflicts of Interest

The authors declare that they have no competing interests.

Authors' Contributions

MFC, TJC, YLG, HMW, WSH, and CYS were responsible for the study conception and design. TJC, HMW, and WSH were responsible for the grant support. YYH and CHC performed the radiopharmaceutical synthesis and quality control. MFC did the animal experiments. MFC and RFY interpreted the microPET images and performed the data analysis. MFC and YYH were major contributors in writing the manuscript. CYS critically reviewed and edited the manuscript for intellectual content. All authors read and approved the final manuscript. Ya-Yao Huang, Wen-Sheng Huang, and Chyng-Yann Shiue contributed equally to this work.

Acknowledgments

We are grateful to Ms. Kwanyu Lin, Ms. Yu-Ning Cheng, Mr. Pei-Yau Lin, and Mr. Chi-Han Wu, for their technical support. This work was supported by the Ministry of Science and Technology of Taiwan (MOST 103-2314-B-002-040-MY3, MOST 105-2314-B-075-060-MY3, and MOST109-2314-B-002-101) and National Taiwan University Hospital (NTUH 109-S4475).

Supplementary Materials

Information on the radiosynthesis and quality control tests are provided. *(Supplementary Materials)*

References

[1] D. J. DiSabato, N. Quan, and J. P. Godbout, "Neuroinflammation: the devil is in the details," *Journal of Neurochemistry*, vol. 139, Suppl 2, pp. 136–153, 2016.

[2] V. Calsolaro and P. Edison, "Neuroinflammation in Alzheimer's disease: current evidence and future directions," *Alzheimers Dement*, vol. 12, no. 6, pp. 719–732, 2016.

[3] R. Troubat, P. Barone, S. Leman et al., "Neuroinflammation and depression: a review," *The European Journal of Neuroscience*, vol. 53, no. 1, pp. 151–171, 2021.

[4] T. R. Marques, A. H. Ashok, T. Pillinger et al., "Neuroinflammation in schizophrenia: meta-analysis of in vivo microglial imaging studies," *Psychological Medicine*, vol. 49, no. 13, pp. 2186–2196, 2019.

[5] L. Meda, M. A. Cassatella, G. I. Szendrei et al., "Activation of microglial cells by β-amyloid protein and interferon-γ," *Nature*, vol. 374, no. 6523, pp. 647–650, 1995.

[6] I. Morales, J. M. Jimenez, M. Mancilla, and R. B. Maccioni, "Tau oligomers and fibrils induce activation of microglial cells," *Journal of Alzheimer's Disease*, vol. 37, no. 4, pp. 849–856, 2013.

[7] R. R. Anholt, E. B. De Souza, M. L. Oster-Granite, and S. H. Snyder, "Peripheral-type benzodiazepine receptors: autoradiographic localization in whole-body sections of neonatal rats," *The Journal of Pharmacology and Experimental Therapeutics*, vol. 233, no. 2, pp. 517–526, 1985.

[8] E. Bribes, D. Carriere, C. Goubet, S. Galiegue, P. Casellas, and J. Simony-Lafontaine, "Immunohistochemical assessment of the peripheral benzodiazepine receptor in human tissues," *The Journal of Histochemistry and Cytochemistry*, vol. 52, no. 1, pp. 19–28, 2004.

[9] D. R. Gehlert, H. I. Yamamura, and J. K. Wamsley, "Autoradiographic localization of "peripheral-type" benzodiazepine binding sites in the rat brain, heart and kidney," *Naunyn-Schmiedeberg's Archives of Pharmacology*, vol. 328, no. 4, pp. 454–460, 1985.

[10] S. Lavisse, M. Guillermier, A. S. Herard et al., "Reactive astrocytes overexpress TSPO and are detected by TSPO positron emission tomography imaging," *The Journal of Neuroscience*, vol. 32, no. 32, pp. 10809–10818, 2012.

[11] H. Wilms, J. Claasen, C. Rohl, J. Sievers, G. Deuschl, and R. Lucius, "Involvement of benzodiazepine receptors in neuroinflammatory and neurodegenerative diseases: evidence from activated microglial cells in vitro," *Neurobiology of Disease*, vol. 14, no. 3, pp. 417–424, 2003.

[12] S. Bradburn, C. Murgatroyd, and N. Ray, "Neuroinflammation in mild cognitive impairment and Alzheimer's disease: a meta-analysis," *Ageing Research Reviews*, vol. 50, pp. 1–8, 2019.

[13] H. Miettinen, J. Kononen, H. Haapasalo et al., "Expression of peripheral-type benzodiazepine receptor and diazepam binding inhibitor in human astrocytomas: relationship to cell proliferation," *Cancer Research*, vol. 55, no. 12, pp. 2691–2695, 1995.

[14] N. Miyazawa, E. Hamel, and M. Diksic, "Assessment of the peripheral benzodiazepine receptors in human gliomas by two methods," *Journal of Neuro-Oncology*, vol. 38, no. 1, pp. 19–26, 1998.

[15] A. Fafalios, A. Akhavan, A. V. Parwani, R. R. Bies, K. J. McHugh, and B. R. Pflug, "Translocator protein blockade reduces prostate tumor growth," *Clinical Cancer Research*, vol. 15, no. 19, pp. 6177–6184, 2009.

[16] Z. Han, R. S. Slack, W. Li, and V. Papadopoulos, "Expression of peripheral benzodiazepine receptor (PBR) in human tumors: relationship to breast, colorectal, and prostate tumor progression," *Journal of Receptor and Signal Transduction Research*, vol. 23, no. 2-3, pp. 225–238, 2003.

[17] Y. Katz, A. Eitan, and M. Gavish, "Increase in peripheral benzodiazepine binding sites in colonic adenocarcinoma," *Oncology*, vol. 47, pp. 139–142, 2004.

[18] I. Königsrainer, U. F. Vogel, S. Beckert et al., "Increased translocator protein (TSPO) mRNA levels in colon but not in rectum carcinoma," *European Surgical Research*, vol. 39, no. 6, pp. 359–363, 2007.

[19] K. Maaser, P. Grabowski, A. P. Sutter et al., "Overexpression of the peripheral benzodiazepine receptor is a relevant prognostic factor in stage III colorectal cancer," *Clinical Cancer Research*, vol. 8, no. 10, pp. 3205–3209, 2002.

[20] A. Beinlich, R. Strohmeier, M. Kaufmann, and H. Kuhl, "Relation of cell proliferation to expression of peripheral benzodiazepine receptors in human breast cancer cell lines," *Biochemical Pharmacology*, vol. 60, no. 3, pp. 397–402, 2000.

[21] S. Galiegue, P. Casellas, A. Kramar, N. Tinel, and J. Simony-Lafontaine, "Immunohistochemical assessment of the peripheral benzodiazepine receptor in breast cancer and its relationship with survival," *Clinical Cancer Research*, vol. 10, no. 6, pp. 2058–2064, 2004.

[22] A. P. Sutter, K. Maaser, M. Höpfner et al., "Specific ligands of the peripheral benzodiazepine receptor induce apoptosis and cell cycle arrest in human esophageal cancer cells," *International Journal of Cancer*, vol. 102, no. 4, pp. 318–327, 2002.

[23] S. Batra and C. S. Iosif, "Peripheral benzodiazepine receptor in human endometrium and endometrial carcinoma," *Anticancer Research*, vol. 20, no. 1A, pp. 463–466, 2000.

[24] I. Venturini, H. Alho, I. Podkletnova et al., "Increased expression of peripheral benzodiazepine receptors and diazepam binding inhibitor in human tumors sited in the liver," *Life Sciences*, vol. 65, no. 21, pp. 2223–2231, 1999.

[25] G. Grande, P. L. S. Ljungman, K. Eneroth, T. Bellander, and D. Rizzuto, "Association between cardiovascular disease and long-term exposure to air pollution with the risk of dementia," *JAMA Neurology*, vol. 77, no. 7, pp. 801–809, 2020.

[26] M. C. Power, M. G. Weisskopf, S. E. Alexeeff, B. A. Coull, A. Spiro III., and J. Schwartz, "Traffic-related air pollution and cognitive function in a cohort of older men," *Environmental Health Perspectives*, vol. 119, no. 5, pp. 682–687, 2011.

[27] B. Ritz, P. C. Lee, J. Hansen et al., "Traffic-related air pollution and Parkinson's disease in Denmark: a case-control study," *Environmental Health Perspectives*, vol. 124, no. 3, pp. 351–356, 2016.

[28] Y. Wang, M. N. Eliot, and G. A. Wellenius, "Short-term changes in ambient particulate matter and risk of stroke: a systematic review and meta-analysis," *Journal of the American Heart Association*, vol. 3, no. 4, 2014.

[29] K. N. Kim, Y. H. Lim, H. J. Bae, M. Kim, K. Jung, and Y. C. Hong, "Long-term fine particulate matter exposure and major depressive disorder in a community-based urban cohort," *Environmental Health Perspectives*, vol. 124, no. 10, pp. 1547–1553, 2016.

[30] M. A. Kioumourtzoglou, M. C. Power, J. E. Hart et al., "The association between air pollution and onset of depression among middle-aged and older women," *American Journal of Epidemiology*, vol. 185, no. 9, pp. 801–809, 2017.

[31] M. L. Block, L. Zecca, and J. S. Hong, "Microglia-mediated neurotoxicity: uncovering the molecular mechanisms," *Nature Reviews. Neuroscience*, vol. 8, no. 1, pp. 57–69, 2007.

[32] A. Campbell, M. Oldham, A. Becaria et al., "Particulate matter in polluted air may increase biomarkers of inflammation in mouse brain," *Neurotoxicology*, vol. 26, no. 1, pp. 133–140, 2005.

[33] J. L. Allen, X. Liu, D. Weston et al., "Developmental exposure to concentrated ambient ultrafine particulate matter air pollution in mice results in persistent and sex-dependent behavioral neurotoxicity and glial activation," *Toxicological Sciences*, vol. 140, no. 1, pp. 160–178, 2014.

[34] M. L. Block and L. Calderon-Garciduenas, "Air pollution: mechanisms of neuroinflammation and CNS disease," *Trends in Neurosciences*, vol. 32, no. 9, pp. 506–516, 2009.

[35] M. K. Chen and T. R. Guilarte, "Translocator protein 18 kDa (TSPO): molecular sensor of brain injury and repair," *Pharmacology & Therapeutics*, vol. 118, no. 1, pp. 1–17, 2008.

[36] J. Choi, M. Ifuku, M. Noda, and T. R. Guilarte, "Translocator protein (18 kDa)/peripheral benzodiazepine receptor specific ligands induce microglia functions consistent with an activated state," *Glia*, vol. 59, no. 2, pp. 219–230, 2011.

[37] R. B. Banati, G. W. Goerres, R. Myers et al., "[11C](R)-PK11195 positron emission tomography imaging of activated microglia in vivo in Rasmussen's encephalitis," *Neurology*, vol. 53, no. 9, pp. 2199–2203, 1999.

[38] F. Chauveau, H. Boutin, N. Van Camp, F. Dolle, and B. Tavitian, "Nuclear imaging of neuroinflammation: a comprehensive review of [11C]PK11195 challengers," *European Journal of Nuclear Medicine and Molecular Imaging*, vol. 35, no. 12, pp. 2304–2319, 2008.

[39] S. Pappata, P. Cornu, Y. Samson et al., "PET study of carbon-11-PK 11195 binding to peripheral type benzodiazepine sites in glioblastoma: a case report," *Journal of Nuclear Medicine*, vol. 32, no. 8, pp. 1608–1610, 1991.

[40] R. Mizrahi, P. M. Rusjan, I. Vitcu et al., "Whole body biodistribution and radiation dosimetry in humans of a new PET

ligand, [(18) F]-FEPPA, to image translocator protein (18 kDa)," *Molecular Imaging and Biology*, vol. 15, no. 3, pp. 353–359, 2013.

[41] P. M. Rusjan, A. A. Wilson, P. M. Bloomfield et al., "Quantitation of translocator protein binding in human brain with the novel radioligand [18F]-FEPPA and positron emission tomography," *Journal of Cerebral Blood Flow and Metabolism*, vol. 31, no. 8, pp. 1807–1816, 2011.

[42] N. Vignal, S. Cisternino, N. Rizzo-Padoin et al., "[(18)F]FEPPA a TSPO radioligand: optimized radiosynthesis and evaluation as a PET radiotracer for brain inflammation in a peripheral LPS-injected mouse model," *Molecules*, vol. 23, no. 6, article 1375, 2018.

[43] A. A. Wilson, A. Garcia, J. Parkes et al., "Radiosynthesis and initial evaluation of [^{18}F]-FEPPA for PET imaging of peripheral benzodiazepine receptors," *Nuclear Medicine and Biology*, vol. 35, no. 3, pp. 305–314, 2008.

[44] Y. Fujimura, Y. Ikoma, F. Yasuno et al., "Quantitative analyses of 18F-FEDAA1106 binding to peripheral benzodiazepine receptors in living human brain," *Journal of Nuclear Medicine*, vol. 47, no. 1, pp. 43–50, 2006.

[45] M. R. Zhang, J. Maeda, K. Furutsuka et al., "[^{18}F]FMDAA1106 and [^{18}F]FEDAA1106: two positron-emitter labeled ligands for peripheral benzodiazepine receptor (PBR)," *Bioorganic & Medicinal Chemistry Letters*, vol. 13, no. 2, pp. 201–204, 2003.

[46] S. S. Golla, R. Boellaard, V. Oikonen et al., "Quantification of [18F]DPA-714 binding in the human brain: initial studies in healthy controls and Alzheimer's disease patients," *Journal of Cerebral Blood Flow and Metabolism*, vol. 35, no. 5, pp. 766–772, 2015.

[47] M. A. Peyronneau, W. Saba, S. Goutal et al., "Metabolism and quantification of [(18)F]DPA-714, a new TSPO positron emission tomography radioligand," *Drug Metabolism and Disposition*, vol. 41, no. 1, pp. 122–131, 2013.

[48] L. P. Dickstein, S. S. Zoghbi, Y. Fujimura et al., "Comparison of 18F- and 11C-labeled aryloxyanilide analogs to measure translocator protein in human brain using positron emission tomography," *European Journal of Nuclear Medicine and Molecular Imaging*, vol. 38, no. 2, pp. 352–357, 2011.

[49] Y. Fujimura, S. S. Zoghbi, F. G. Simeon et al., "Quantification of translocator protein (18 kDa) in the human brain with PET and a novel radioligand, (18)F-PBR06," *Journal of Nuclear Medicine*, vol. 50, no. 7, pp. 1047–1053, 2009.

[50] D. Ory, S. Celen, A. Verbruggen, and G. Bormans, "PET radioligands for in vivo visualization of neuroinflammation," *Current Pharmaceutical Design*, vol. 20, no. 37, pp. 5897–5913, 2014.

[51] L. Zhang, K. Hu, T. Shao et al., "Recent developments on PET radiotracers for TSPO and their applications in neuroimaging," *Acta Pharmaceutica Sinica B*, vol. 11, no. 2, pp. 373–393, 2021.

[52] W. F. Chau, A. M. Black, A. Clarke et al., "Exploration of the impact of stereochemistry on the identification of the novel translocator protein PET imaging agent [^{18}F]GE-180," *Nuclear Medicine and Biology*, vol. 42, no. 9, pp. 711–719, 2015.

[53] Z. Fan, V. Calsolaro, R. A. Atkinson et al., "Flutriciclamide (18F-GE180) PET: first-in-human PET study of novel third-generation in vivo marker of human translocator protein," *Journal of Nuclear Medicine*, vol. 57, no. 11, pp. 1753–1759, 2016.

[54] T. Wickstrøm, A. Clarke, I. Gausemel et al., "The development of an automated and GMP compliant FASTlab synthesis of [(18) F]GE-180; a radiotracer for imaging translocator protein (TSPO)," *Journal of Labelled Compounds and Radiopharmaceuticals*, vol. 57, no. 1, pp. 42–48, 2014.

[55] K. J. Langen and A. Willuweit, "TSPO PET using 18F-GE-180: a new perspective in neurooncology?," *European Journal of Nuclear Medicine and Molecular Imaging*, vol. 44, no. 13, pp. 2227–2229, 2017.

[56] P. Zanotti-Fregonara, M. Veronese, B. Pascual, R. C. Rostomily, F. Turkheimer, and J. C. Masdeu, "The validity of 18F-GE180 as a TSPO imaging agent," *European Journal of Nuclear Medicine and Molecular Imaging*, vol. 46, no. 6, pp. 1205–1207, 2019.

[57] P. Zanotti-Fregonara, B. Pascual, G. Rizzo et al., "Head-to-head comparison of11C-PBR28 and18F-GE180 for quantification of the translocator protein in the human brain," *Journal of Nuclear Medicine*, vol. 59, no. 8, pp. 1260–1266, 2018.

[58] N. Vasdev, D. E. Green, D. C. Vines et al., "Positron-emission tomography imaging of the TSPO with [(18)F]FEPPA in a preclinical breast cancer model," *Cancer Biotherapy & Radiopharmaceuticals*, vol. 28, no. 3, pp. 254–259, 2013.

[59] M. Zammit, Y. Tao, M. E. Olsen et al., "[18F]FEPPA PET imaging for monitoring CD68-positive microglia/macrophage neuroinflammation in nonhuman primates," *EJNMMI Research*, vol. 10, no. 1, pp. 1–12, 2020.

[60] S. Attwells, E. Setiawan, P. M. Rusjan et al., "Translocator protein distribution volume predicts reduction of symptoms during open-label trial of celecoxib in major depressive disorder," *Biological Psychiatry*, vol. 88, no. 8, pp. 649–656, 2020.

[61] S. Attwells, E. Setiawan, A. A. Wilson et al., "Inflammation in the neurocircuitry of obsessive-compulsive disorder," *JAMA Psychiatry*, vol. 74, no. 8, pp. 833–840, 2017.

[62] T. Da Silva, S. Hafizi, J. J. Watts et al., "In vivo imaging of translocator protein in long-term Cannabis users," *JAMA Psychiatry*, vol. 76, no. 12, pp. 1305–1313, 2019.

[63] S. Hafizi, H. H. Tseng, N. Rao et al., "Imaging microglial activation in untreated first-episode psychosis: a PET study with [18F]FEPPA," *The American Journal of Psychiatry*, vol. 174, no. 2, pp. 118–124, 2017.

[64] S. V. Hartimath, S. Khanapur, R. Boominathan et al., "Imaging adipose tissue browning using the TSPO-18kDa tracer [^{18}F]FEPPA," *Molecular Metabolism*, vol. 25, pp. 154–158, 2019.

[65] E. Setiawan, A. A. Wilson, R. Mizrahi et al., "Role of translocator protein density, a marker of neuroinflammation, in the brain during major depressive episodes," *JAMA Psychiatry*, vol. 72, no. 3, pp. 268–275, 2015.

[66] R. Yilmaz, A. P. Strafella, A. Bernard et al., "Serum inflammatory profile for the discrimination of clinical subtypes in Parkinson's disease," *Frontiers in Neurology*, vol. 9, p. 1123, 2018.

[67] USP, "Monographs: fludeoxyglucose F 18 injection," 2015.

[68] S. H. Lee, P. H. Lee, H. J. Liang et al., "Brain lipid profiles in the spontaneously hypertensive rat after subchronic real-world exposure to ambient fine particulate matter," *Science of The Total Environment*, vol. 707, p. 135603, 2020.

[69] Y. H. Yan, C. C. K. Chou, J. S. Wang et al., "Subchronic effects of inhaled ambient particulate matter on glucose homeostasis and target organ damage in a type 1 diabetic rat model," *Toxicology and Applied Pharmacology*, vol. 281, no. 2, pp. 211–220, 2014.

[70] H. C. Chuang, H. C. Chen, P. J. Chai et al., "Neuropathology changed by 3- and 6-months low-level PM2.5 inhalation

exposure in spontaneously hypertensive rats," *Particle and Fibre Toxicology*, vol. 17, pp. 1–12, 2020.

[71] R. Boellaard, "Standards for PET image acquisition and quantitative data analysis," *Journal of Nuclear Medicine*, vol. 50, Suppl 1, pp. 11S–20S, 2009.

[72] K. J. Bai, K. J. Chuang, C. L. Chen et al., "Microglial activation and inflammation caused by traffic-related particulate matter," *Chemico-Biological Interactions*, vol. 311, p. 108762, 2019.

[73] N. Berroterán-Infante, T. Balber, P. Furlinger et al., "[18F]FEPPA: improved automated radiosynthesis, binding affinity, and preliminary in vitro evaluation in colorectal cancer," *ACS Medicinal Chemistry Letters*, vol. 9, no. 3, pp. 177–181, 2018.

[74] C. W. Chang, C. H. Chiu, M. H. Lin et al., "GMP-compliant fully automated radiosynthesis of [18F]FEPPA for PET/MRI imaging of regional brain TSPO expression," *EJNMMI Research*, vol. 11, no. 1, p. 26, 2021.

[75] V. Narayanaswami, J. Tong, C. Schifani, P. M. Bloomfield, K. Dahl, and N. Vasdev, "Preclinical evaluation of TSPO and MAO-B PET radiotracers in an LPS model of neuroinflammation," *PET Clinics*, vol. 16, no. 2, pp. 233–247, 2021.

[76] Y. W. Young, C. V. Barback, L. A. Stolz et al., "MicroPET evidence for a hypersensitive neuroinflammatory profile of gp120 mouse model of HIV," *Psychiatry Research: Neuroimaging*, vol. 321, p. 111445, 2022.

[77] E. Setiawan, S. Attwells, A. A. Wilson et al., "Association of translocator protein total distribution volume with duration of untreated major depressive disorder: a cross-sectional study," *Lancet Psychiatry*, vol. 5, no. 4, pp. 339–347, 2018.

[78] M. Kenk, T. Selvanathan, N. Rao et al., "Imaging neuroinflammation in gray and white matter in schizophrenia: an in-vivo PET study with [18F]-FEPPA," *Schizophrenia Bulletin*, vol. 41, no. 1, pp. 85–93, 2015.

[79] I. Suridjan, B. G. Pollock, N. P. Verhoeff et al., "_In-vivo_ imaging of grey and white matter neuroinflammation in Alzheimer 's disease: a positron emission tomography study with a novel radioligand, [^{18}F]-FEPPA," *Molecular Psychiatry*, vol. 20, no. 12, pp. 1579–1587, 2015.

[80] N. U. Al-Khishman, Q. Qi, A. D. Roseborough et al., "TSPO PET detects acute neuroinflammation but not diffuse chronically activated MHCII microglia in the rat," *EJNMMI Research*, vol. 10, no. 1, pp. 1–10, 2020.